Molecular mechanisms of invadopodium formation: the role of the N-WASP–Arp2/3 complex pathway and cofilin

Hideki Yamaguchi,[1,3] Mike Lorenz,[1] Stephan Kempiak,[1] Corina Sarmiento,[1] Salvatore Coniglio,[5] Marc Symons,[1,2] Jeffrey Segall,[1] Robert Eddy,[1] Hiroaki Miki,[3,6] Tadaomi Takenawa,[4,7] and John Condeelis[1]

[1]Department of Anatomy and Structural Biology and [2]Department of Surgery, Albert Einstein College of Medicine, Bronx, NY 10461
[3]Department of Cancer Genomics and [4]Department of Biochemistry, Institute of Medical Science, University of Tokyo, Tokyo 108-8639, Japan
[5]Center for Oncology and Cell Biology, North Shore-Long Island Jewish Research Institute, Manhasset, NY 11030
[6]Precursory Research for Embryonic Science and Technology and [7]Core Research for Evolutional Science and Technology, Japan Science and Technology Corporation, Tokyo 108-8639, Japan

Invadopodia are actin-rich membrane protrusions with a matrix degradation activity formed by invasive cancer cells. We have studied the molecular mechanisms of invadopodium formation in metastatic carcinoma cells. Epidermal growth factor (EGF) receptor kinase inhibitors blocked invadopodium formation in the presence of serum, and EGF stimulation of serum-starved cells induced invadopodium formation. RNA interference and dominant-negative mutant expression analyses revealed that neural WASP (N-WASP), Arp2/3 complex, and their upstream regulators, Nck1, Cdc42, and WIP, are necessary for invadopodium formation. Time-lapse analysis revealed that invadopodia are formed de novo at the cell periphery and their lifetime varies from minutes to several hours. Invadopodia with short lifetimes are motile, whereas long-lived invadopodia tend to be stationary. Interestingly, suppression of cofilin expression by RNA interference inhibited the formation of long-lived invadopodia, resulting in formation of only short-lived invadopodia with less matrix degradation activity. These results indicate that EGF receptor signaling regulates invadopodium formation through the N-WASP–Arp2/3 pathway and cofilin is necessary for the stabilization and maturation of invadopodia.

Introduction

Metastasis, a process in which tumor cells spread to another organ, is the most feared property of malignant cancer cells. For cancer cells to metastasize, they must first detach from the parent tumor and invade and migrate into surrounding connective tissue and blood vessels (Chambers et al., 2002). This invasion of cancer cells is induced by chemoattractants, such as EGF, that diffuse from blood vessels and get secreted from other cell types, including macrophages (Condeelis and Segall, 2003; Wyckoff et al., 2004). The initial step of cancer cell migration and invasion is the extension of cell protrusions in the direction of cell movement (Friedl and Wolf, 2003). The formation of these cell protrusions is driven by actin polymerization at the leading edge (Pollard and Borisy, 2003). Malignant tumor cells often show excessive cell protrusive activity due to aberrant activation of signaling pathways that regulate actin cytoskeletal rearrangement (Wang et al., 2004).

Invadopodia are membrane protrusions with a matrix degradation activity formed by invasive cancer cells (Chen, 1989). These structures extend vertically from the ventral cell membrane into the ECM. In tumors, invadopodia-like structures are believed to be important for tumor cells to penetrate the basement membrane of blood vessels (Condeelis and Segall, 2003). Invadopodia are enriched with actin filaments, actin binding proteins, adhesion proteins, matrix proteinases, and signaling proteins that regulate the actin cytoskeleton and membrane remodeling (Buccione et al., 2004; McNiven et al., 2004). However, molecular mechanisms that govern assembly and dynamics of invadopodia are still not well understood.

WASP (Wiskott-Aldrich syndrome protein) family proteins are key regulators of the actin cytoskeleton (Miki and Takenawa, 2003; Stradal et al., 2004). To date, five family members, WASP, neural WASP (N-WASP), WAVE1 (WASP

Correspondence to John Condeelis: condeeli@aecom.yu.edu

Abbreviations used in this paper: CBD, cortactin-binding domain; FN, fibronectin; N-WASP, neural WASP; RNAi, RNA interference; siRNA, small interference RNA; WBD, N-WASP binding domain.

The online version of this article includes supplemental material.

The Journal of Cell Biology, Vol. 168, No. 3, January 31, 2005 441–452
http://www.jcb.org/cgi/doi/10.1083/jcb.200407076

family verprolin-homologous protein 1), WAVE2, and WAVE3, have been described. WASP family proteins are implicated in a variety of cellular processes associated with dynamic actin structures, such as the formation of membrane protrusions, vesicular trafficking, and the intracellular motility of several pathogens. All WASP family proteins have a conserved COOH-terminal region termed the VCA (verprolin homology, cofilin homology or central, and acidic) domain. This catalytic domain induces actin polymerization through the activation of the Arp2/3 (actin-related protein 2 and 3) complex (Millard et al., 2004). The Arp2/3 complex nucleates actin filaments and forms a branched actin filament network observed in lamellipodia. Several signaling molecules, such as Nck, Grb2, WISH (WASP-interacting SH3 protein), Cdc42, and phosphoinositides, have been shown to activate N-WASP by releasing it from the autoinhibitory conformation. Nck recruits N-WASP protein to the active site of actin polymerization through WIP (WASP-interacting protein; Moreau et al., 2000). Several groups reported that WASP, N-WASP, and Arp2/3 complex are components of podosomes, similar structures to invadopodia (Linder et al., 1999; Mizutani et al., 2002; Kaverina et al., 2003). Also, recent results with an N-WASP biosensor demonstrated that N-WASP is activated at the cell membrane during the initiation of invadopodium formation, thereby implicating N-WASP activity in the initiation of invasion (Lorenz et al., 2004b). However, functions of these proteins in invadopodia remain to be determined.

Cofilin is a critical regulator of actin dynamics and protrusive activity in cells. Cofilin nucleates actin polymerization by severing actin filaments to generate free barbed ends (Condeelis, 2001). Cofilin also increases the rate of actin depolymerization, thus maintaining a pool of actin monomer (Carlier et al., 1999). Previous studies showed that cofilin stimulates lamellipod protrusion and cell migration (Chan et al., 2000; Dawe et al., 2003; Ghosh et al., 2004). Moreover, cofilin is one of the essential components for in vitro reconstitution of *Listeria monocytogenes* motility that is driven by actin polymerization (Loisel et al., 1999). The function of cofilin in invadopodium formation has not yet been studied.

Recent studies using DNA microarrays have revealed that a subset of proteins involved in the rearrangement of the actin cytoskeleton is overexpressed in metastatic cancer cells. For example, the N-WASP gene has been identified to be upregulated in metastatic lesions of colorectal cancers (Yanagawa et al., 2001). Moreover, the invasive population of tumor cells in mammary tumors expresses, at elevated levels, components of the pathways that regulate actin polymerization at the leading edge, including Cdc42, Arp2/3 complex subunits, and cofilin (Wang et al., 2004). However, little is known about the role of N-WASP, Arp2/3 complex, and cofilin in the acquisition of invasive phenotypes by cancer cells.

Here, we report the functional analyses of the N-WASP–Arp2/3 complex pathway and cofilin in invasiveness of MTLn3 rat adenocarcinoma cells. We found that N-WASP and the Arp2/3 complex have a role in the formation of invadopodia induced by the EGF receptor signaling. Cdc42, Nck1, and WIP are necessary for invadopodium formation among upstream regulators of N-WASP. Interestingly, cofilin is not necessary for invadopodium formation, but is required for maturation of fully functional invadopodia.

Results

Characterization of invadopodium formation in rat mammary carcinoma cells

When cultured on Alexa488-labeled fibronectin (FN) and gelatin-coated dishes, MTLn3 cells, highly metastatic rat mammary adenocarcinoma cells, formed punctate structures rich in actin filaments at the ventral cell membrane (Fig. 1 A). Z sectioning by confocal microscopy revealed that these structures protruded vertically from the ventral membrane into FN matrix. These protrusions were often associated with sites of FN degradation that were detected as black holes in the Alexa488 channel and were positive for cortactin, an actin binding protein known to localize at invadopodia (Fig. 1 B). These properties of the actin dot structures are clearly consistent with that of invadopodia reported previously (Buccione et al., 2004; McNiven et al., 2004).

We examined the correlation between invadopodium formation and metastatic potential of cancer cells. MTC cells were

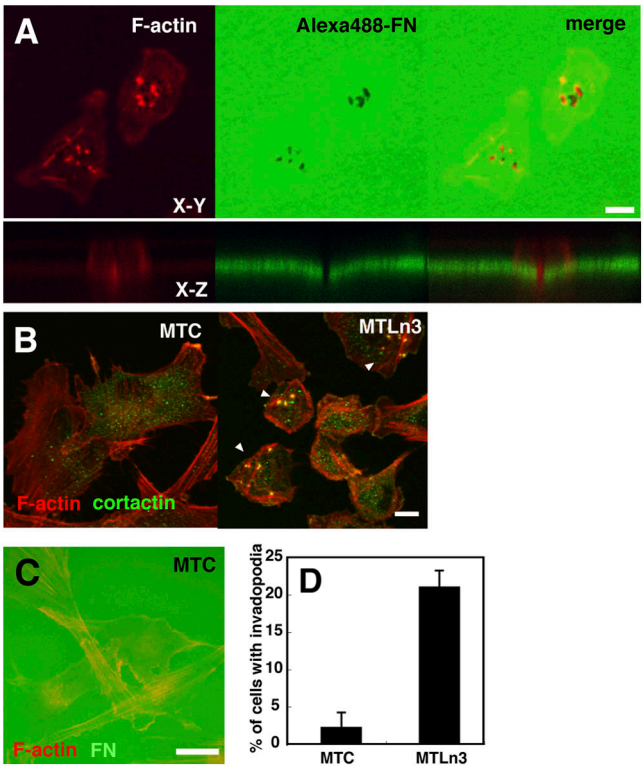

Figure 1. **Metastatic MTLn3 cells but not nonmetastatic MTC cells form invadopodia.** (A) MTLn3 cells cultured on Alexa488-FN– and gelatin-coated glass coverslips were stained with rhodamine phalloidin. Bottom images are XZ sections showing a cell with an invadopodium collected with a confocal microscope. Bar, 10 μm. (B) MTC and MTLn3 cells grown on FN- and gelatin-coated coverslips were stained with anti-cortactin antibody and phalloidin. Arrowheads indicate cells displaying invadopodia. Bar, 20 μm. (C) MTC cells cultured on Alexa488-FN (green)– and gelatin-coated glass coverslips were stained with rhodamine phalloidin (red). Bar, 10 μm. (D) The percentage of cells with invadopodia in MTC and MTLn3 cells was calculated as described in Materials and methods. Error bars represent the SD of three different determinations.

derived from the same breast tumor as MTLn3 cells, but these cells are less invasive and nonmetastatic, as revealed by in vitro invasion assays and animal model experiments (Neri et al., 1982; Wyckoff et al., 2000b). MTC cells were cultured on Alexa488 FN-gelatin dishes and examined for invadopodium formation. MTC cells showed well elongated and spread morphology on the FN-gelatin dish compared with MTLn3 cells. However, invadopodium formation and degradation of FN were hardly observed in these cells (Fig. 1, B and C). To quantitate invadopodium formation, the number of cells with cortactin-positive invadopodia was calculated (Fig. 1 D). Approximately 21% of MTLn3 cells and only 2% of MTC cells showed invadopodium formation.

Time-lapse analysis of invadopodia

To study the assembly mechanism of invadopodia, we performed time-lapse microscopy with MTLn3 cells stably expressing GFP- or YFP-actin cultured on the FN-gelatin dishes. Invadopodia often arise at the cell periphery (Fig. 2 A and Video 1, available at http://www.jcb.org/cgi/content/full/jcb.200407076/DC1). Most invadopodia were formed de novo, and few invadopodia showed fission or fusion behavior. Surprisingly, invadopodia were motile; some of them moved around on the ventral cell membrane and then disappeared within minutes, whereas others first showed motile behavior and then arrested, remaining in the same position for hours (Fig. 2 A, a–c). When invadopodia became stationary, they were often associated with halo-like actin clouds that surround an actin-rich core of invadopodia (Fig. 2 A, a). When the fluorescence intensity of GFP-actin of an invadopodium is plotted versus the speed of its movement between frames as a function of time, there is a significant inverse correlation between the intensity and the speed of the invadopodium (Fig. 2 C). This result suggests that motile invadopodia are associated with fewer actin filaments than stable invadopodia. Interestingly, we repeatedly observed that long-lived stable invadopodia were left

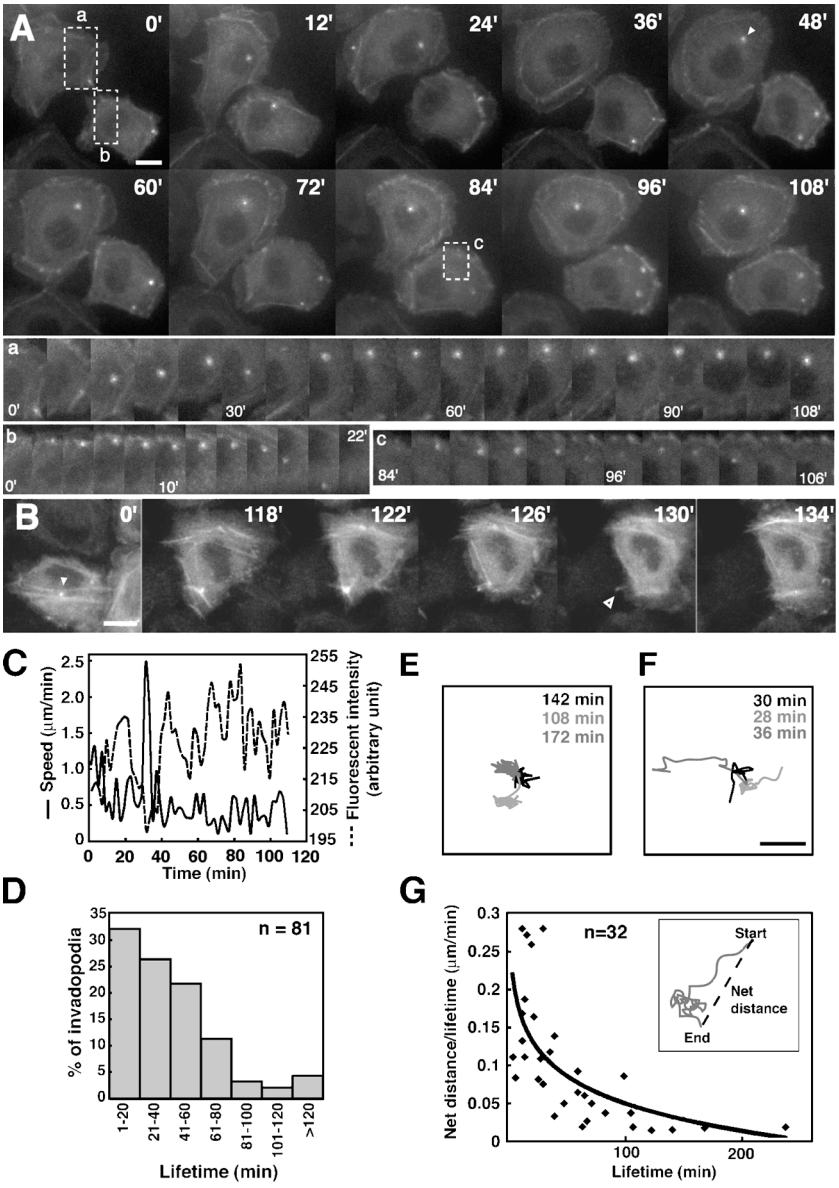

Figure 2. **Time-lapse analysis of invadopodium formation.** (A) Time-lapse image sequence of MTLn3 cells expressing GFP-actin. Cells were cultured on FN-gelatin–coated coverslips and analyzed by automated time-lapse microscopy. The invadopodium denoted by an arrowhead is stationary, whereas invadopodia in the lower right cell are dynamic. Bar, 10 μm. (a–c) Time-lapse image sequences of boxed regions. (B) Time-lapse image sequence showing a long-lived stationary invadopodium (closed arrowhead). Open arrowhead denotes an invadopodium left behind by a moving cell. Bar, 10 μm. (C) The fluorescence intensity of the invadopodium shown in Fig. 2 A (a) was plotted versus the speed of its movement as a function of time. The inverse correlation between the fluorescence intensity and the speed indicates that actin polymerization occurs in invadopodia when they become stationary. (D) Distribution of the lifetimes of invadopodia shown in histogram. (E and F) The trajectories of representative long-lived (E) and short-lived (F) invadopodia are shown as lines. The lifetime of each invadopodium is also shown in the box. Bar, 5 μm. (G) Net distance moved by each invadopodium was calculated as shown in the inset and divided by its lifetime, and the ratio was plotted versus lifetime. The ratio is expected to be lower if invadopodia are more stationary. The data indicate that long-lived invadopodia are more stationary than short-lived invadopodia.

behind when cells moved away, resulting in formation of a tail-like membrane structure (Fig. 2 B and Video 2, available at http://www.jcb.org/cgi/content/full/jcb.200407076/DC1), indicating that they have a strong contact with the substrate, protruding into the ECM.

We then measured the lifetime and movement of invadopodia. The lifetime of invadopodia varies from a few minutes up to several hours (Fig. 2 D). Tracking analysis of invadopodia movement showed that invadopodia with longer lifetimes have a tendency to stay at one spot and are less motile than short-lived invadopodia (Fig. 2, E and F). This observation was confirmed by dividing the net distance moved for each invadopodium by its lifetime and plotting that ratio versus lifetime (Fig. 2 G). The ratio is expected to be lower if invadopodia are more stationary. The result is consistent with the hypothesis that long-lived invadopodia derive from motile precursors and they are stationary because they are protruded into matrix.

EGF and the EGF receptor signaling are necessary for the formation of invadopodia

EGF is a well-known growth factor that induces dynamic cell protrusions associated with the actin cytoskeleton. The difference in invasive potential between MTLn3 and MTC cells is at least partly due to different responsiveness to EGF. MTLn3 but not MTC cells show chemotaxis to EGF as observed both in culture and tumors (Bailly et al., 1998; Wyckoff et al., 2000a). Therefore, we examined the importance of EGF receptor signaling in invadopodium formation.

MTLn3 cells were cultured on the FN-gelatin dishes in the presence of serum with or without an EGF receptor kinase inhibitor, AG1478. AG1478 treatment inhibited formation of invadopodia in a dose-dependent manner (Fig. 3 A). As shown in Fig. 3 C, MTLn3 cells formed lamellipodia and stress fibers even after treatment with AG1478, suggesting that in serum, invadopodia are more dependent on EGF receptor signaling than other actin structures. Similar results were obtained with two other EGF receptor kinase inhibitors, PD153035 and Iressa (Fig. S1, available at http://www.jcb.org/cgi/content/full/jcb.200407076/DC1). We tested if EGF stimulation is sufficient to induce invadopodium formation in MTLn3 cells. After serum starvation, MTLn3 cells grown on FN-gelatin dishes were stimulated with EGF. Serum starvation markedly reduced invadopodium formation (Fig. 3, B and D). Stimulation with EGF induced extension of lamellipodia as well as formation of actin dot-like structures that were observed at the basal membrane and positive for cortactin staining (Fig. 3 D). The EGF-induced formation of invadopodia was blocked by preincubation of cells with AG1478 (Fig. 3 B).

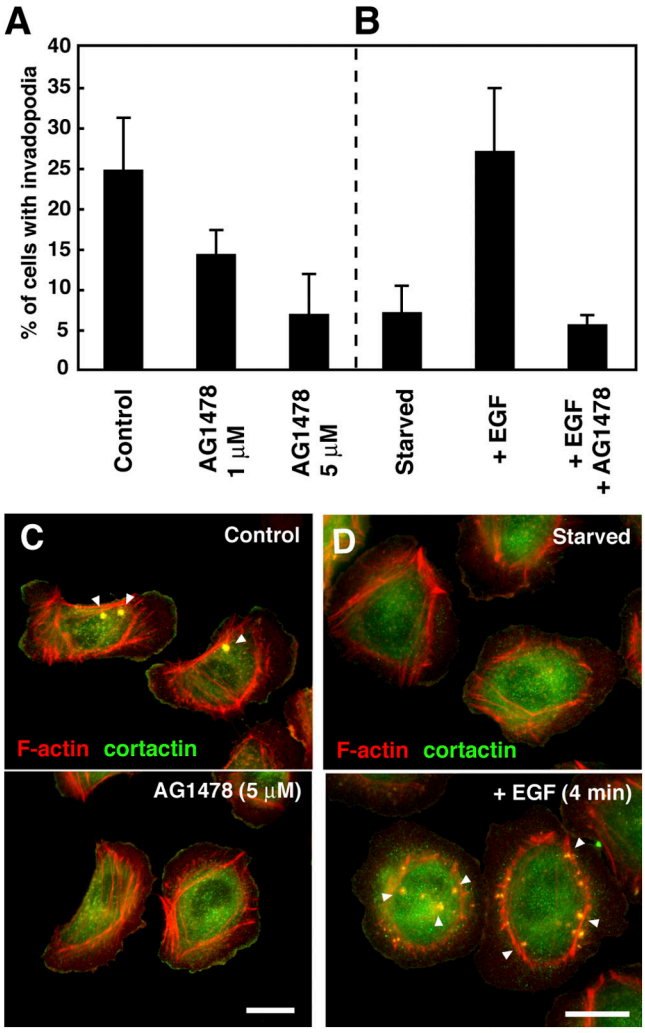

Figure 3. **EGF and EGF receptor signaling are necessary for invadopodium formation.** (A) Effect of an EGF receptor kinase inhibitor AG1478 on invadopodium formation. Cells were cultured on FN-gelatin coverslips in the presence of serum with or without AG1478 for 16 h. Cells were then stained with rhodamine phalloidin and anti-cortactin antibody to quantitate invadopodium formation. (B) Effect of serum starvation and subsequent EGF stimulation on invadopodium formation. Cells cultured on FN-gelatin coverslips were serum starved for 4 h with or without 5 μM AG1478 and stimulated with 12.5 nM EGF for 4 min. Error bars represent the SD of three different determinations. (C) Morphology of cells treated with AG1478. After treatment with AG1478 in the presence of serum, cells were stained with rhodamine phalloidin and anti-cortactin antibody. Cells formed stress fibers and lamellipodia even after AG1478 treatment. (D) Morphology of cells serum starved and stimulated with EGF. Arrowheads denote invadopodia. Bars, 10 μm.

Localization of WASP family proteins and the Arp2/3 complex at invadopodia

WASP family proteins have been reported to induce de novo actin polymerization through activation of the Arp2/3 complex in response to extracellular stimuli including EGF stimulation. Thus, we next examined the localization of N-WASP and other WASP family proteins, WAVE1 and WAVE2, along with the downstream effecter Arp2/3 complex at invadopodia (Fig. 4). WAVE3 expression was undetectable in cultured MTLn3 cells by RT-PCR analysis (Fig. S2, available at http://www.jcb.org/cgi/content/full/jcb.200407076/DC1). N-WASP staining was clearly concentrated at invadopodia. WAVE1 staining was very dim in these cells and showed no specific localization. Strong staining for WAVE2 was seen in the cytoplasm and nucleus and at the leading edges of lamellipodia, but not at invadopodia. p34arc, a subunit of the Arp2/3 complex, localized at invadopodia as well as at the leading edges of lamellipodia. A similar staining pattern was obtained

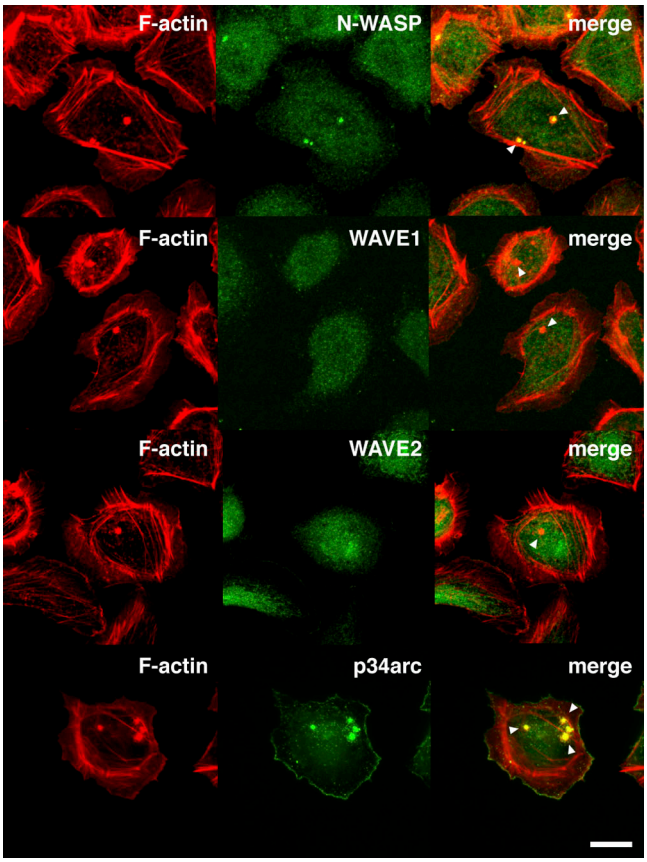

Figure 4. **Localization of WASP family proteins and Arp2/3 complex at invadopodia.** Cells grown on FN-gelatin–coated coverslips were stained with anti-N-WASP, anti-WAVE1, anti-WAVE2, or anti-p34arc antibody. To visualize actin filaments, the cells were also stained with rhodamine phalloidin. Arrowheads denote invadopodia. Bar, 10 μm.

with an antibody against Arp2, another subunit of the Arp2/3 complex (unpublished data). These results indicate that N-WASP is specifically localized at invadopodia together with the Arp2/3 complex, whereas the WAVE proteins are not.

N-WASP and the Arp2/3 complex are essential components of invadopodia

We assessed the involvement of N-WASP and the Arp2/3 complex in invadopodium formation. RNA interference (RNAi) was performed to reduce expression of N-WASP, WAVE1, WAVE2, and p34arc, and reduction of protein expression was confirmed by immunoblotting (Fig. 5 A). In N-WASP small interference RNA (siRNA)–treated cells, the N-WASP expression level was reduced to ∼30% of control cells. The expression of WAVE1 was reduced to <30% of control cells by siRNA treatment, and WAVE2 and p34arc expression were hardly detected in the siRNA-treated cells. Cells treated with N-WASP siRNA showed a reduction of invadopodium formation but no inhibition of lamellipodium formation (Fig. 5, B and C). This effect of N-WASP siRNA was rescued by ectopic expression of bovine GFP-N-WASP that has mismatches in the N-WASP siRNA target sequence (Fig. 5 C). Similar inhibition of invadopodium formation was observed in cells transfected with a dominant-negative mutant (Δcof) of N-WASP that lacks the sequence required for efficient Arp2/3 complex binding and activation (Banzai et al., 2000; Fig. 5 D). Overexpression of the N-WASP CA domain that dislocates the Arp2/3 complex and p34arc siRNA treatment also resulted in inhibition of invadopodium formation (Fig. 5, B, C, and E). In contrast, WAVE1 and WAVE2 siRNA-treated cells formed invadopodia as efficiently as control cells (Fig. 5, B and C). Degradation activity of the siRNA-treated cells correlated with invadopodium formation, except for WAVE1 siRNA (Fig. S3, available at http://www.jcb.org/cgi/content/full/jcb.200407076/DC1). WAVE1 siRNA-treated cells showed a significant decrease in degradation activity, although formation of invadopodia looked normal. This result may be due to the decreased secretion of MMP-2, an ECM-degrading metalloproteinase and a component of invadopodia (Chen and Wang, 1999), by WAVE1 knock down as reported previously (Suetsugu et al., 2003). Together, these results indicate that N-WASP and the Arp2/3 complex, but not WAVE1 and 2, are required for formation of invadopodia and that WAVE1 has an indirect role in matrix degradation.

Nck1, but not Grb2, is necessary for invadopodium formation

Several upstream activators, including Nck, Grb2, Cdc42, WIP, and WISH, have been shown to regulate N-WASP activation. Also, these proteins are known to mediate the EGF receptor signaling pathway–dependent reorganization of the actin cytoskeleton. Therefore, we analyzed the importance of these upstream activators of N-WASP in invadopodium formation.

First, we examined the localization of Nck1 and Grb2 at invadopodia by expressing GFP-fusion proteins (Fig. 6 A). GFP-Nck1 accumulated at invadopodia, and to a lesser extent at focal adhesions. In contrast, GFP-Grb2 was seen throughout the cytoplasm and not localized at invadopodia. Then, we performed targeted depletion of Nck1 and Grb2 by RNAi. Both Nck and Grb2 protein levels were reduced to <10% of the control level after siRNA treatment in immunoblotting (Fig. 6 B). Because we used an antibody against Nck that recognizes both Nck1 and Nck2, the immunoblotting result demonstrates that Nck1 is the major isoform in MTLn3 cells. Invadopodium formation in Nck1 siRNA-treated cells was markedly suppressed, whereas Grb2 siRNA treatment had little effect (Fig. 6 C). Degradation activity was also inhibited by Nck1 siRNA treatment (Fig. S3). Ectopic expression of human GFP-Nck1 partially restored invadopodium formation in Nck1 siRNA-treated cells (Fig. 6 C). Nck2 may account for the residual invadopodium formation in Nck1siRNA-treated cells. Indeed, expression of Nck2 was detected in MTLn3 cells (Fig. S2). We tried Nck2 knock down by RNAi in this assay but it was not informative with regard to invadopodium formation due to impairment of cell adhesion and spreading on the matrix in Nck2 knockdown cells.

Cdc42 and WIP are crucial regulators of invadopodium formation

The importance of Cdc42 was examined by reducing its expression by RNAi. Cells were transfected with siRNA designed against the Cdc42 gene and tested for invadopodium formation. Knock down of Cdc42 protein was confirmed by immunoblot-

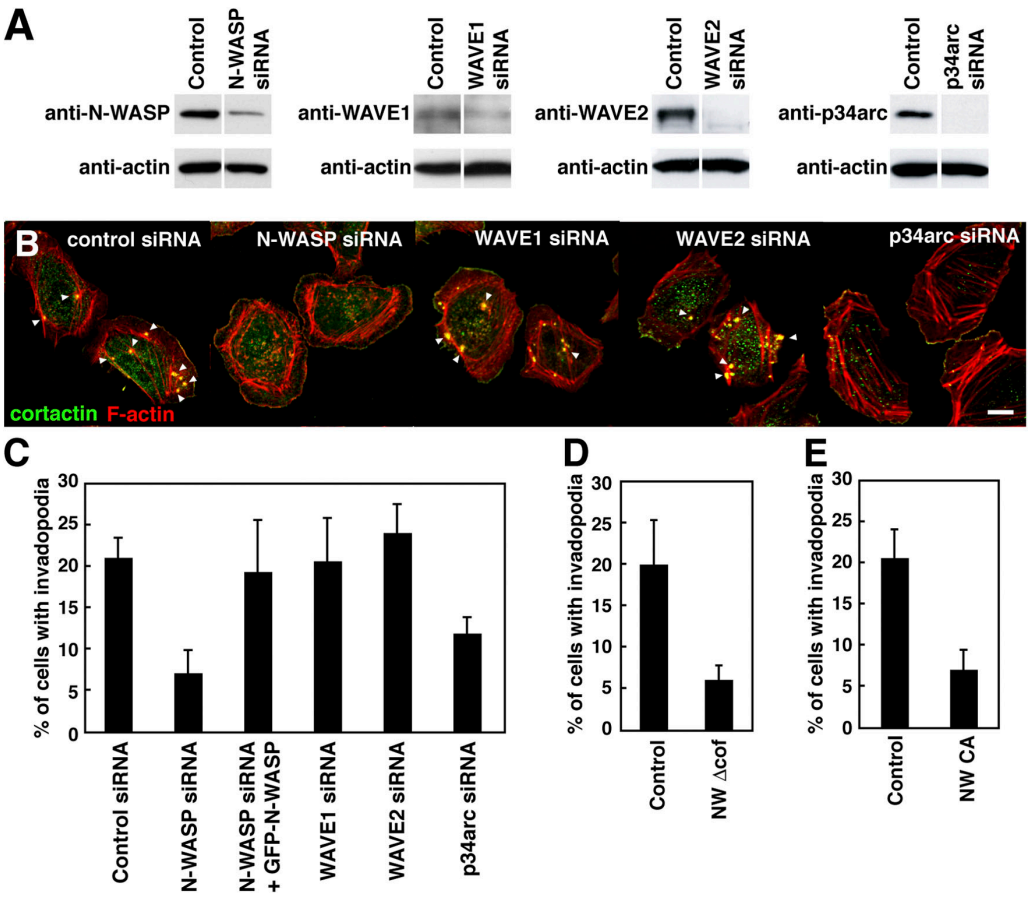

Figure 5. **N-WASP and Arp2/3 complex are involved in invadopodium formation.** (A) Cells were transfected with control, N-WASP, WAVE1, WAVE2, or p34arc siRNA. Cell lysates were prepared at 48 h after transfection and immunoblotted with the indicated antibodies. Anti-actin antibody was used for loading controls. (B) Cells treated with siRNAs were stained with anti-cortactin and rhodamine phalloidin to visualize invadopodia (arrowheads). Bar, 10 μm. (C) Invadopodium formation in cells treated with siRNAs. For rescue experiments, N-WASP siRNA-treated cells were transfected with the bovine GFP-N-WASP construct. (D) Invadopodium formation in cells infected with retroviruses expressing control GFP or dominant-negative N-WASP (NW Δcof). (E) Cells were transfected with control GFP or GFP-N-WASP CA constructs, and invadopodium formation was quantified. Error bars represent the SD of three different determinations.

ting lysates prepared from cells treated with control or Cdc42 siRNA (Fig. 7 A). Cells treated with Cdc42 siRNA showed a nearly complete inhibition of invadopodium formation (Fig. 7, B and C). Similar inhibition was observed in cells transfected with dominant-negative Cdc42 (Fig. S4, available at http://www.jcb.org/cgi/content/full/jcb.200407076/DC1). Thus, Cdc42 activity is required for invadopodium formation.

Next, we tested whether or not WIP is involved in the formation of invadopodia. WIP is thought to link Nck and N-WASP to induce actin polymerization (Moreau et al., 2000; Benesch et al., 2002). MTLn3 cells were transfected with GFP-tagged wild-type WIP or the N-WASP binding domain (WBD) of WIP that disrupts the interaction between N-WASP and WIP (Moreau et al., 2000). Wild-type GFP-WIP significantly accumulated at invadopodia (Fig. 7 D). Cells expressing GFP-WBD showed a marked reduction in invadopodium formation (Fig. 7, D and E). Because WIP was also shown to associate with cortactin, a central component of invadopodia (Kinley et al., 2003), we tested the importance of the WIP–cortactin interaction by overexpressing a WIP fragment containing the cortactin-binding domain (CBD). GFP-CBD signals were observed at invadopodia, and its expression showed little effect on invadopodium formation (Fig. 7, D and E). These results demonstrate that WIP–N-WASP interaction is necessary for invadopodium formation but not WIP–cortactin interaction.

WISH is an N-WASP binding protein that is able to fully activate N-WASP independently of Cdc42 (Fukuoka et al., 2001). WISH expression in MTLn3 cells was confirmed by RT-PCR (Fig. S2). GFP-tagged wild-type and ΔSH3 mutant of WISH proteins were overexpressed in MTLn3 cells. The ΔSH3 mutant of WISH lacks the N-WASP binding site, therefore this mutant is supposed to act as a dominant-negative mutant. Wild-type GFP-WISH was observed at invadopodia (Fig. 7 F). Interestingly, WISH ΔSH3 also accumulated at invadopodia, indicating that localization of WISH at invadopodia is independent of N-WASP binding. Concurrently, invadopodium formation was not affected by overexpression of wild-type or ΔSH3 WISH (Fig. 7 G). These results suggest that WISH–N-WASP binding is dispensable for invadopodium formation.

Suppression of cofilin expression results in the formation of short-lived, less invasive invadopodia

We previously reported that cofilin is necessary for lamellipod protrusion induced by EGF in MTLn3 cells (Chan et al., 2000; DesMarais et al., 2004). Therefore, we investigated if cofilin

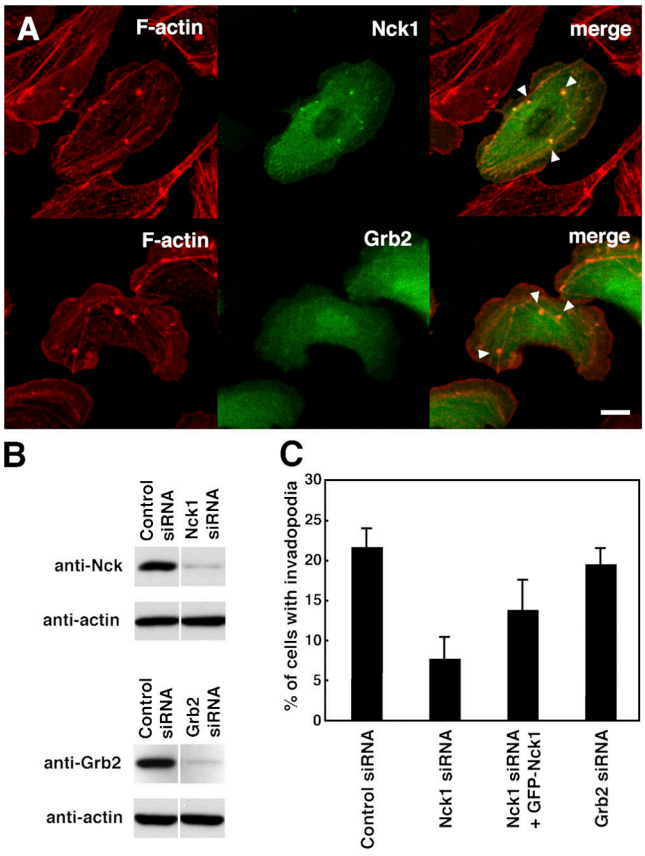

Figure 6. **Nck1 but not Grb2 is required for formation of invadopodia.** (A) Cells transfected with GFP-Nck1 or Grb2 construct were stained with rhodamine phalloidin to visualize invadopodia (arrowheads). Bar, 10 μm. (B) Cells were transfected with control, Nck1, or Grb2 siRNA. Cell lysates were immunoblotted with anti-Nck, anti-Grb2, and anti-actin antibodies. (C) Invadopodia formation was quantified among cells treated with indicated siRNAs. Nck1 siRNA-treated cells were transfected with human GFP-Nck1 construct for rescue experiment. Error bars represent the SD of three different determinations.

has a role in formation of invadopodia. Localization of endogenous cofilin was examined by immunostaining with antcofilin antibody (Fig. 8 A). Strong cofilin staining was observed at the leading edge of lamellipodia, and cofilin was also localized at invadopodia. Cofilin function was investigated by knocking down cofilin expression by RNAi. The siRNA used was shown to be specific for cofilin by rescue experiments (Ghosh et al., 2004). Cofilin expression in the siRNA-treated cells was suppressed at least by 80% (Fig. 8 B). Cofilin siRNA-treated cells had an elongated morphology and were still capable of forming cortactin-positive invadopodia, although these invadopodia looked smaller than those in control cells (Fig. 8 C). Quantitative analysis revealed only a small but significant decrease in invadopodium formation in cofilin siRNA-treated cells (Fig. 8 D). The matrix degradation activity of cofilin knockdown cells was also examined. Interestingly, cofilin siRNA-treated cells showed less ability to invade and degrade matrix than control cells (Fig. 8 E and Fig. S3). This result raised the possibility that cofilin is required for maturation of invadopodia. To test this possibility, time-lapse analysis was performed with YFP-actin cells treated with control or cofilin siRNA. This analysis clearly demonstrated that the lifetime of invadopodia was shortened by cofilin siRNA treatment as compared with control cells (Fig. 8 F). The number of cells with invadopodia with lifetimes <20 min was increased, whereas the number with lifetimes >30 min was decreased. Together, these results indicate that cofilin has a role in the stabilization and/or maturation process of invadopodia rather than in the initiation process.

Discussion

Cells use two kinds of protrusions, filopodia and lamellipodia, to migrate forward in two-dimensional culture. In addition to these structures, invasive cancer cells can form another type of protrusive structure, the invadopodium that is associated with ECM degradation. Considering that most tumor cells are surrounded by ECM in vivo, invadopodia may be major protrusive structures formed by cancer cells in the three-dimensional physiological environment.

N-WASP and Arp2/3 complex in invadopodium formation

In this work, we demonstrate that N-WASP and Arp2/3 complex but not WAVE1 and WAVE2 are required for invadopodium formation by highly invasive and metastatic cancer cells. This finding is consistent with N-WASP biosensor experiments showing transient N-WASP activity in invadopodia (Lorenz et al., 2004b). Additionally, localization of N-WASP at invadopodia was also observed in other human cancer cell lines including HT1080 fibrosarcoma and RPMI7951 melanoma cells (unpublished data). These observations suggest that N-WASP functions in invadopodium formation in a broad range of cancer cell types. We demonstrated that highly metastatic MTLn3 cells but not nonmetastatic MTC cells can form invadopodia, indicating a direct correlation between the ability to form invadopodia and metastatic potential of cancer cells. Coopman et al. (1998) also showed a relationship between the localized degradation of ECM by invadopodia and invasive capacity of human breast cancer cell lines. Therefore, invadopodia-related molecules, such as N-WASP and Arp2/3 complex, could be therapeutic targets of cancer metastasis. Additionally, our results also indicate that N-WASP is involved in the protrusion of invadopodia but not lamellipodia. This is consistent with the observation that N-WASP–deficient fibroblasts can form lamellipodia normally (Snapper et al., 2001). These results suggest that N-WASP is important for specialized focal protrusive structures and not broad protrusive activity involved in cell locomotion.

Nck, Cdc42, and WIP mediate EGF receptor signaling to invadopodium formation

In many different cancer cell types the prognosis of a patient is inversely correlated with the overexpression and/or amplification of the EGF receptor family (Nicholson et al., 2001). Accumulating evidence suggests that EGF receptor ligands and the EGF receptor signaling pathway are critical for the invasiveness and metastasis of cancer cells. Indeed, EGF receptor inhibitors have been shown to inhibit invasive po-

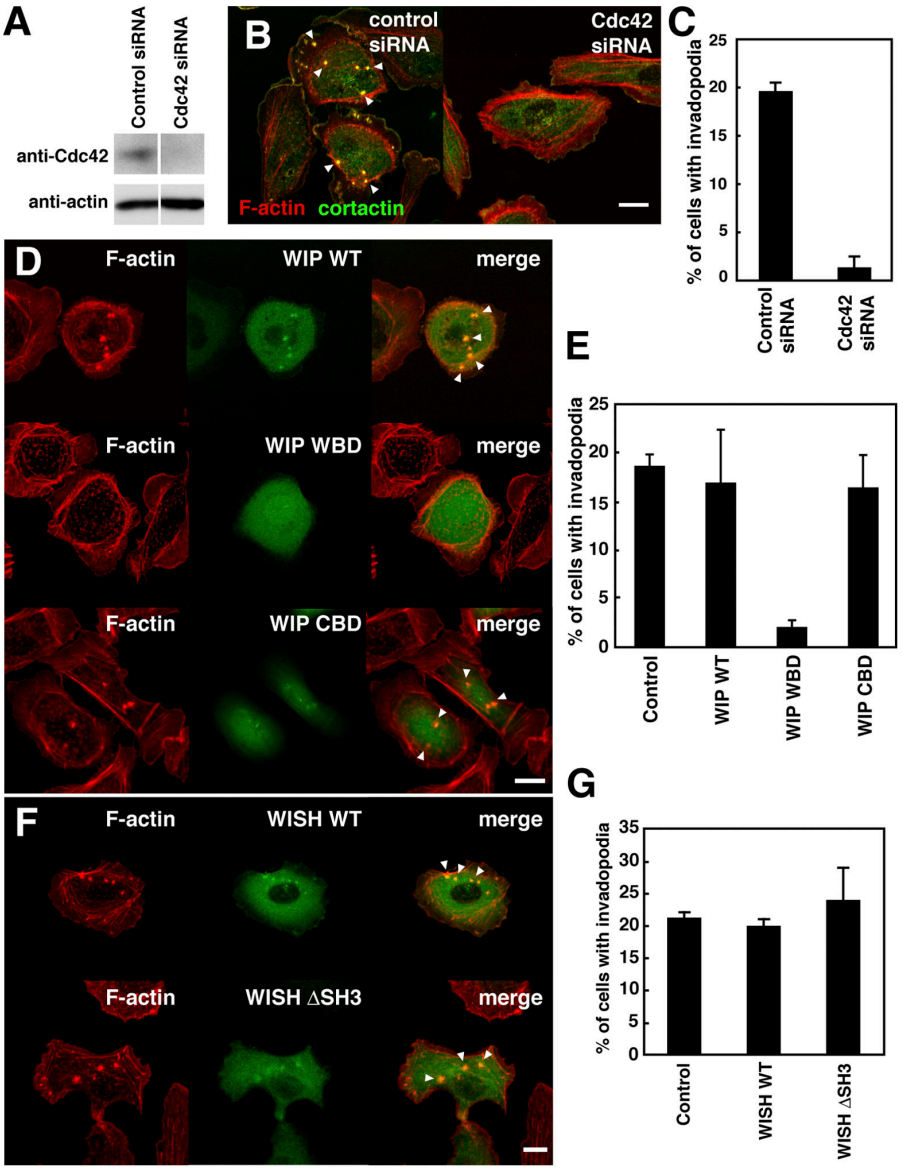

Figure 7. **Cdc42 and WIP–N-WASP interaction are essential for invadopodium formation.** (A) Cells were transfected with control or Cdc42 siRNA, and the cell lysates were immunoblotted with anti-Cdc42 and anti-actin antibodies. Cdc42 was not detected in cells treated with Cdc42 siRNA. (B) Cells treated with control or Cdc42 siRNA were stained with anti-cortactin and rhodamine phalloidin to visualize invadopodia. (C) Invadopodia formation was quantified among cells transfected with control or Cdc42 siRNA. (D) Cells transfected with GFP-tagged WIP wild type (WT), N-WASP binding domain (WBD), or cortactin binding domain (CBD) construct were stained with rhodamine phalloidin. (E) Invadopodia formation was quantified among transfected cells. (F) Cells expressing GFP-tagged wild-type WISH (WT) or WISH mutant lacking SH3 domain (ΔSH3) were stained with rhodamine phalloidin. (G) Quantitation of invadopodium formation. Error bars represent the SD of three different determinations. Arrowheads denote invadopodia. Bars, 10 μm.

tency of cancer cells (Fujimura et al., 2002; Yang et al., 2004). In this paper, we showed that EGF receptor signaling is necessary for invadopodium formation. Therefore, invadopodium formation may be an initial key step of cancer cell invasion and metastasis induced by activation of EGF receptor signaling.

EGF receptor activation stimulates signaling pathways that lead to enhancement of cell growth and cell motility. N-WASP is known to be activated downstream of the EGF receptor through Cdc42 and/or adaptor proteins including Grb2, Nck, WIP, and WISH. Additionally, activation of Cdc42 was observed after EGF stimulation in MTLn3 cells (unpublished data). We report here that Nck1, Cdc42, and WIP, but not Grb2 and WISH, are crucial for invadopodium formation. Cdc42 was also shown to function in invadopodium formation in human melanoma cells (Nakahara et al., 2003). Rohatgi et al. (2001) showed that Nck activates N-WASP in vitro, and, interestingly, Nck and Cdc42 have redundant effects on N-WASP activity. Therefore, it is unlikely that both Nck and Cdc42 directly bind to and activate N-WASP simultaneously at invadopodia. Nck and/or Cdc42 might have other effecters that regulate invadopodium formation, such as PAK, a well-characterized Nck and Cdc42 downstream effecter that has been implicated in cytoskeletal dynamics and cell motility. However, PAK activity was not important for invadopodium formation (Fig. S5 A, available at http://www.jcb.org/cgi/content/full/jcb.200407076/DC1). An alternative possibility is that Cdc42 regulates N-WASP activity indirectly through Toca-1 (transducer of Cdc42-dependent actin assembly), a novel regulator of Cdc42-dependent actin polymerization (Ho et al., 2004). Toca-1 links Cdc42 activity to N-WASP by direct binding to both molecules. Notably, Ho et al. (2004) also showed that most of N-WASP proteins are complexed with WIP in bovine brain and *Xenopus laevis* eggs, and this complex formation is required for proper regulation of N-WASP activity by Toca-1. Consistent with this, we also detected an interaction between N-WASP and WIP in MTLn3 cells, but this interaction was

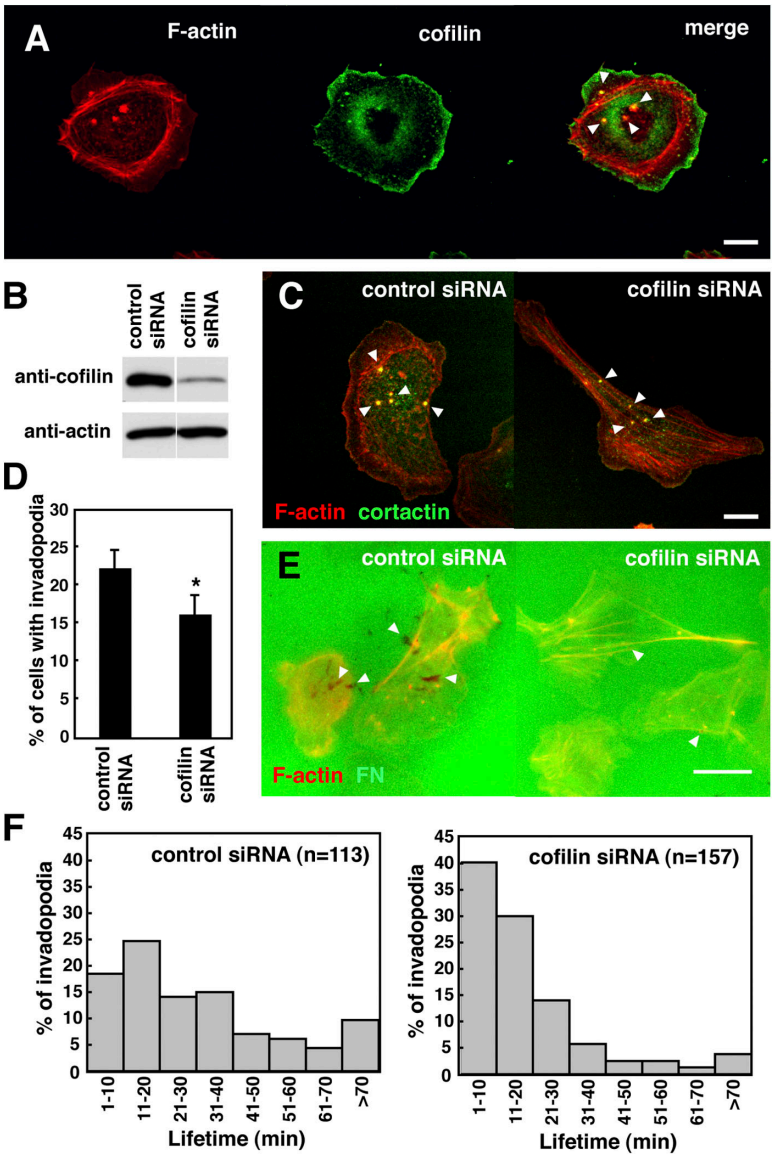

Figure 8. **Cofilin is required for fully functional invadopodia.** (A) Cells grown on FN-gelatin–coated coverslips were stained with anti-cofilin antibody and rhodamine phalloidin. Arrowheads denote invadopodia. (B) Cells were transfected with control or cofilin siRNA, and the cell lysates were immunoblotted with anti-cofilin and anti-actin antibodies. (C) Cells treated with control or cofilin siRNA were stained with anti-cortactin antibody and rhodamine phalloidin. Arrowheads denote invadopodia. (D) Invadopodia formation was quantified among cells transfected with control or cofilin siRNA. Error bars represent the SD of three different determinations. Asterisk denotes statistical significance ($P < 0.04$) compared with control calculated by *t* test. (E) Cells treated with control or cofilin siRNA were cultured on Alexa488-FN– and gelatin-coated glass coverslips to analyze their degradation activity. The cells were stained with rhodamine phalloidin. Arrowheads denote the degradation sites. (F) MTLn3 cells expressing YFP-actin were transfected with control or cofilin siRNA and analyzed by time-lapse microscopy. Lifetime of invadopodia was calculated from the time-lapse movies and shown in histograms. Bars, 10 μm.

unchanged upon EGF stimulation (Fig. S5 B), indicating that the N-WASP–WIP complex is constitutive in MTLn3 cells. Collectively, Nck1 may recruit the N-WASP–WIP complex to the site of invadopodium formation upon EGF stimulation, and Cdc42 indirectly activates N-WASP through Toca-1 to initiate invadopodium assembly. Also, it is possible that Nck and Cdc42 regulate N-WASP activity in succession at different stages of invadopodium formation. Further work would be necessary to define the exact upstream signals that regulate N-WASP activation at invadopodia.

Invadopodia and podosomes

Podosomes are highly dynamic actin-rich adhesion structures formed by cells of monocytic lineage such as macrophages and osteoclasts and by other cell types including certain transformed fibroblasts and smooth muscle cells (Linder and Aepfelbacher, 2003). Podosomes are enriched in regulatory proteins for the actin cytoskeleton, including Cdc42 and WIP (Moreau et al., 2003) and adhesion proteins (McNiven et al., 2004). Podosomes formed by transformed fibroblasts are capable of degrading ECM (Mizutani et al., 2002). Therefore, podosomes and invadopodia share similarities in appearance and molecular composition. However, recent studies have revealed several significant differences between these structures in structure and function (Baldassarre et al., 2003). For example, podosomes are tubular invaginations of the ventral plasma membrane (Ochoa et al., 2000), whereas invadopodia are membrane protrusions extending into the ECM that originate from the large invagination of the ventral plasma membrane without evidence of inward tubulations. It has been proposed that podosomes could be precursor structures that mature into invadopodia under the appropriate physiological conditions (Baldassarre et al., 2003; Linder and Aepfelbacher, 2003), although direct experimental evidence for this hypothesis has not been available.

In this work, we performed for the first time a time-lapse analysis of invadopodium formation. This analysis revealed that there are significant differences between podosomes and

invadopodia in terms of their dynamics: (a) invadopodia are mainly formed de novo at the cell periphery around lamellipodia. Evans et al. (2003) reported that macrophage podosomes assemble also at the leading lamella, but mainly by fragmentation of preexisting precursors. Therefore, assembly mechanisms seem to differ between invadopodia and macrophage podosomes. (b) Invadopodia have lifetimes varying from a few minutes to hours, whereas the lifetime of podosomes was reported to be several minutes (Destaing et al., 2003; Evans et al., 2003). (c) Invadopodia are motile structures. In contrast, it was reported that net movement of podosome clusters is achieved by continuous formation of podosomes at the front and disassembly at the rear, and individual podosomes are not motile (Destaing et al., 2003).

We found that there are roughly two types of invadopodia, short-lived motile invadopodia and stationary long-lived invadopodia. The stationary invadopodia appear to have a strong contact with the substrate, suggesting that they protrude into matrix and execute matrix degradation. Additionally, it was often observed that long-lived invadopodia moved around after formation and then became stationary. Therefore, the short-lived motile invadopodia appear to be precursors of fully functional invadopodia. Given that the lifetime of podosome is several minutes, podosomes might be equivalent to the short-lived invadopodia observed in this paper. However, there are still some differences between these two structures as described in the previous paragraph. These differences could be caused by the use of different substrates for analysis because most studies of podosome function have been performed on nonphysiological substrates such as glass. Also, it is possible that the organization and dynamics of invadopodia/podosomes are cell type dependent. Therefore, more detailed analyses will be necessary to understand the relationship between invadopodia and podosomes.

Function of cofilin in invadopodium formation

We found that suppression of cofilin expression by siRNA results in the formation of small, less invasive invadopodia with short lifetimes. These results suggest that cofilin principally functions in the maturation of invadopodia, rather than the initiation of invadopodium assembly. We often observed that long-lived stationary invadopodia have strong actin signals and are associated with actin clouds indicative of a burst of actin polymerization, suggesting that actin polymerization is required for maturation of invadopodia. Recent studies have demonstrated that Arp2/3 complex and cofilin synergize to induce barbed end formation that drives EGF-induced lamellipodia protrusion (DesMarais et al., 2004). Therefore, cofilin and Arp2/3 complex activity may induce a burst of actin polymerization that is required for invadopodium protrusion, producing stabilization and subsequent maturation.

A model for invadopodium formation

In summary, we propose a model for invadopodium formation (Fig. 9, A and B). Invadopodia are assembled at the cell periphery around lamellipodia de novo. Formation of invadopodia can be triggered by activation of the EGF receptor. Nck1 and Cdc42 are recruited and/or activated downstream of the EGF receptor. Nck1 recruits the N-WASP–WIP complex to the sites of invadopodium formation, and Cdc42 may activate N-WASP through Toca-1. Activated N-WASP induces actin polymerization through Arp2/3 complex that drives invadopodium initiation. These newly formed invadopodia are motile and move laterally at the ventral surface of the cell until additional stimuli induce stabilization. This process requires polymerization of an actin network at the base of invadopodia to anchor these structures. Cofilin may be required for optimizing Arp2/3 complex–mediated dendritic nucleation to cause elongation of the invadopodia and its stabilization.

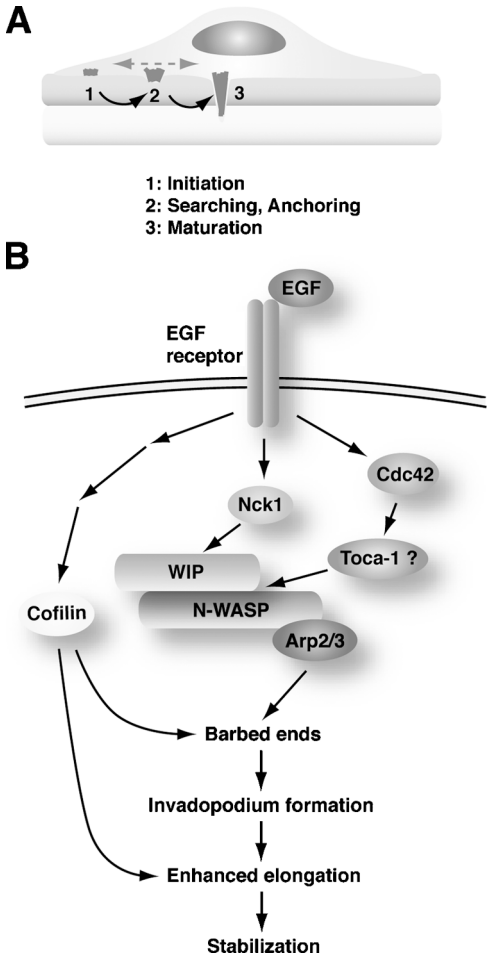

Figure 9. **Model for invadopodium formation.** (A) A model for invadopodium formation. Mature invadopodia are formed through three processes. (1) In the initiation phase, precursors of invadopodia are formed de novo at the cell periphery around lamellipodia. (2) These precursors are motile and move around on the ventral membrane until they stick to ECM. (3) In the maturation phase, anchored invadopodia protrude into ECM and degrade it. (B) Schematic diagram of the signaling pathway for invadopodium formation. EGF ligand binding to the EGF receptor activates and/or recruits Nck1 and Cdc42. Nck1 recruits WIP–N-WASP complex, and Cdc42 activates N-WASP probably through Toca-1 to initiate invadopodium formation. Cofilin mainly functions in the maturation process of invadopodium formation.

Materials and methods

Cell culture
MTLn3 and MTC cells are derived from the 13762NF rat mammary adenocarcinoma. Cells were cultured in α-MEM supplemented with 5% FBS and antibiotics and stimulated with EGF as described previously (Segall et al., 1996).

Antibodies and constructs
Anti–N-WASP and anti-cofilin antibodies have been described previously (Miki et al., 1996; Chan et al., 2000). Anti-WAVE1 and -WAVE2 antibodies were provided by S. Suetsugu and D. Yamazaki (Institute of Medical Science, University of Tokyo, Tokyo, Japan) and described previously (Yamazaki et al., 2003). Anti-p34 and anti-Grb2 antibodies were purchased from Upstate Biotechnology, and anti–β-actin antibody was purchased from Sigma-Aldrich. Anti-Cdc42 antibody was obtained from Santa Cruz Biotechnology, Inc. Anti-Nck antibody is a gift from T. Pawson (Samuel Lunenfeld Research Institute, Mount Sinai Hospital, Toronto, Canada). GFP-Nck1, Grb2, WIP, and WIP WBD constructs are a gift from M. Way (Cancer Research UK, London, UK). For GFP-tagged WISH constructs, cDNAs encoding full-length mouse WISH and ΔSH3 mutant (154–711 aa) that were provided by M. Fukuoka (Institute of Medical Science, University of Tokyo, Tokyo, Japan) were cloned into pEGFP-C1 vector (CLONTECH Laboratories, Inc.). For retroviral construct, cDNA encoding dominant-negative N-WASP (Δcof; Banzai et al., 2000) was ligated into pMX plasmid vector. For bovine GFP-N-WASP construct, bovine N-WASP cDNA was ligated into pEGFP-C1 vector. For WIP CBD construct, cDNA encoding a WIP sequence (124–223 aa) was amplified by RT-PCR from total RNA extracted from MTLn3 cells, and then subcloned into pEGFP-C1 vector.

Invadopodium assay
Fluorescent matrix-coated dishes were prepared as described previously (Chen, 1989). Alexa488 protein labeling kit (Molecular Probes) was used for labeling FN (Sigma-Aldrich). Cells were cultured on the FN-gelatin–coated dishes for 8 to 16 h. For quantitation of invadopodium formation, cells were stained with anti-cortactin antibody and phalloidin. The cells were scored as invadopodium positive if dot-like structures containing both actin filaments and cortactin were present at the basal membrane. Error bars in all figures represent the SD of three different determinations. At least 100 cells were counted in each determination.

Transfection
MTLn3 cells were transfected with indicated plasmids using Lipofectamine 2000 (Invitrogen). Cells were plated at 70% confluence to 6-well plate, and the next day they were incubated with 2 μg DNA and 4 μl Lipofectamine 2000 in OPTI-MEM (Invitrogen) for 45 min. After extensive wash with complete medium, cells were cultured in complete medium for 24 h. The cells were then replated onto FN-gelatin dishes and cultured for an additional 16 h before being analyzed. Retroviral transfection was performed as described previously (Miki et al., 1998).

RNAi
Control, nonsilencing siRNA (AATTCTCCGAACGTGTCACGT) was purchased from QIAGEN. N-WASP siRNA (AAGACGAGATGCTCCAAATGG), WAVE1 siRNA (AATGCCTCCGTCCCCACCTTC), WAVE2 siRNA (AAGGAATCAACACTCGTAAGG), p34arc siRNA (AAGGAACTTCAGGCACACGGA), Grb2 siRNA (AACATCCGTGTCCAGGAACCA), and Nck1 siRNA (GATGATAGCTTTGTTGATCCA) were purchased from Ambion. Cdc42 siRNA (AAAGACTCCTTTCTTGCTTGT) was purchased from Dharmacon. All aforementioned sequences are target rat gene sequences used to design each siRNA. Cofilin siRNA was described previously (Mouneimne et al., 2004). MTLn3 cells were transfected with 100 nM siRNA (WAVE2 siRNA, 50 nM; Cdc42 siRNA, 30 nM) using Oligofectamine (Invitrogen). The cells were cultured for 32 h and then replated onto a FN-gelatin dish for 16 h before being analyzed. For rescue experiments, bovine GFP-N-WASP and human GFP-Nck1 constructs were transfected as described in the previous section at 24 h after siRNA transfection. For immunoblotting, cell lysates were prepared at 48 h after siRNA transfection.

Immunofluorescence
Cells were fixed in 3.7% formaldehyde for 15 min, permeabilized with 0.1% Triton X-100 for 10 min, and blocked in 1% BSA and 1% FBS for 30 min. For cofilin staining, cells were fixed in 3.7% formaldehyde, 0.1% glutaraldehyde, and 0.075 mg/ml saponin for 1 h. The cells were incubated with primary antibodies for 1 h, and then with fluorophore-conjugated secondary antibodies and rhodamine phalloidin (Molecular Probes) for 30 min. The cells were treated with 1 mg/ml sodium borohydrate in PBS for 10 min to quench autofluorescence of residual glutaraldehyde that was used to cross-link gelatin film. All samples were observed with a microscope (Olympus) equipped with a cooled CCD camera or with a confocal laser-scanning microscope (model Radiance 2000; Bio-Rad Laboratories). The images were processed with Adobe Photoshop.

Immunoblotting
Cells were washed with ice-cold PBS before direct extraction in SDS-PAGE sample buffer. The samples were resolved by SDS-PAGE, transferred to nitrocellulose membrane, and blocked in 5% nonfat dried milk. The membranes were incubated with primary antibodies for 1 h, and followed by incubation with peroxidase-conjugated secondary antibodies for 30 min. Immunoreactive bands were detected using a ECL-plus kit (Amersham Biosciences).

Time-lapse microscopy
MTLn3 cells stably expressing YFP- or GFP-actin were used as described previously (Lorenz et al., 2004a). In brief, time-lapse series of the cells were taken at 37°C using a microscope (model 470; Olympus) equipped with a computer-driven cooled CCD camera, humidified CO_2 chamber, and autofocus system and operated by IPlab Spectrum software (VayTek). Phase and fluorescence images were taken every 2 min for up to 16 h. Digital images were converted in NIH image, and lifetime, fluorescence intensity, and motion of invadopodia were analyzed.

Online supplemental material
Fig. S1 shows inhibition of invadopodium formation by EGF receptor kinase inhibitors. Fig. S2 shows RT-PCR analysis of Nck, WISH, and WAVE expression. Degradation activity of siRNA-treated cells is shown in Fig. S3. Function of Cdc42 in invadopodia was analyzed in Fig. S4. Involvement of PAK in invadopodium formation was examined in Fig. S5 A. Fig. S5 B shows interaction of WIP with N-WASP. Video 1 shows dynamics of invadopodia. Video 2 shows an invadopodium with long lifetime. Online supplemental material is available at http://www.jcb.org/cgi/content/full/jcb.200407076/DC1.

We are grateful to Dr. M. Way for Nck, Grb2, and WIP constructs and Dr. T. Pawson for anti-Nck antibody. We thank Drs. S. Suetsugu and D. Yamazaki for anti-WAVE antibodies and Dr. M. Fukuoka for WISH constructs.

This work was supported by grants from the National Institutes of Health (C38511) to J. Condeelis.

Submitted: 12 July 2004
Accepted: 16 December 2004

References

Bailly, M., L. Yan, G.M. Whitesides, J.S. Condeelis, and J.E. Segall. 1998. Regulation of protrusion shape and adhesion to the substratum during chemotactic responses of mammalian carcinoma cells. *Exp. Cell Res.* 241: 285–299.

Baldassarre, M., A. Pompeo, G. Beznoussenko, C. Castaldi, S. Cortellino, M.A. McNiven, A. Luini, and R. Buccione. 2003. Dynamin participates in focal extracellular matrix degradation by invasive cells. *Mol. Biol. Cell.* 14:1074–1084.

Banzai, Y., H. Miki, H. Yamaguchi, and T. Takenawa. 2000. Essential role of neural Wiskott-Aldrich syndrome protein in neurite extension in PC12 cells and rat hippocampal primary culture cells. *J. Biol. Chem.* 275: 11987–11992.

Benesch, S., S. Lommel, A. Steffen, T.E. Stradal, N. Scaplehorn, M. Way, J. Wehland, and K. Rottner. 2002. Phosphatidylinositol 4,5-biphosphate (PIP2)-induced vesicle movement depends on N-WASP and involves Nck, WIP, and Grb2. *J. Biol. Chem.* 277:37771–37776.

Buccione, R., J.D. Orth, and M.A. McNiven. 2004. Foot and mouth: podosomes, invadopodia and circular dorsal ruffles. *Nat. Rev. Mol. Cell Biol.* 5:647–657.

Carlier, M.F., F. Ressad, and D. Pantaloni. 1999. Control of actin dynamics in cell motility. Role of ADF/cofilin. *J. Biol. Chem.* 274:33827–33830.

Chambers, A.F., A.C. Groom, and I.C. MacDonald. 2002. Dissemination and growth of cancer cells in metastatic sites. *Nat. Rev. Cancer.* 2:563–572.

Chan, A.Y., M. Bailly, N. Zebda, J.E. Segall, and J.S. Condeelis. 2000. Role of cofilin in epidermal growth factor–stimulated actin polymerization and lamellipod protrusion. *J. Cell Biol.* 148:531–542.

Chen, W.T. 1989. Proteolytic activity of specialized surface protrusions formed at rosette contact sites of transformed cells. *J. Exp. Zool.* 251:167–185.

Chen, W.T., and J.Y. Wang. 1999. Specialized surface protrusions of invasive cells, invadopodia and lamellipodia, have differential MT1-MMP, MMP-2, and TIMP-2 localization. *Ann. NY Acad. Sci*. 878:361–371.

Condeelis, J. 2001. How is actin polymerization nucleated in vivo? *Trends Cell Biol.* 11:288–293.

Condeelis, J., and J.E. Segall. 2003. Intravital imaging of cell movement in tumours. *Nat. Rev. Cancer.* 3:921–930.

Coopman, P.J., M.T. Do, E.W. Thompson, and S.C. Mueller. 1998. Phagocytosis of cross-linked gelatin matrix by human breast carcinoma cells correlates with their invasive capacity. *Clin. Cancer Res.* 4:507–515.

Dawe, H.R., L.S. Minamide, J.R. Bamburg, and L.P. Cramer. 2003. ADF/cofilin controls cell polarity during fibroblast migration. *Curr. Biol*. 13:252–257.

DesMarais, V., F. Macaluso, J. Condeelis, and M. Bailly. 2004. Synergistic interaction between the Arp2/3 complex and cofilin drives stimulated lamellipod extension. *J. Cell Sci.* 117:3499–3510.

Destaing, O., F. Saltel, J.C. Geminard, P. Jurdic, and F. Bard. 2003. Podosomes display actin turnover and dynamic self-organization in osteoclasts expressing actin-green fluorescent protein. *Mol. Biol. Cell.* 14:407–416.

Evans, J.G., I. Correia, O. Krasavina, N. Watson, and P. Matsudaira. 2003. Macrophage podosomes assemble at the leading lamella by growth and fragmentation. *J. Cell Biol.* 161:697–705.

Friedl, P., and K. Wolf. 2003. Tumour-cell invasion and migration: diversity and escape mechanisms. *Nat. Rev. Cancer.* 3:362–374.

Fujimura, M., T. Hidaka, and S. Saito. 2002. Selective inhibition of the epidermal growth factor receptor by ZD1839 decreases the growth and invasion of ovarian clear cell adenocarcinoma cells. *Clin. Cancer Res.* 8:2448–2454.

Fukuoka, M., S. Suetsugu, H. Miki, K. Fukami, T. Endo, and T. Takenawa. 2001. A novel neural Wiskott-Aldrich syndrome protein (N-WASP) binding protein, WISH, induces Arp2/3 complex activation independent of Cdc42. *J. Cell Biol.* 152:471–482.

Ghosh, M., X. Song, G. Mouneimne, M. Sidani, D.S. Lawrence, and J.S. Condeelis. 2004. Cofilin promotes actin polymerization and defines the direction of cell motility. *Science.* 304:743–746.

Ho, H.Y., R. Rohatgi, A.M. Lebensohn, M. Le, J. Li, S.P. Gygi, and M.W. Kirschner. 2004. Toca-1 mediates Cdc42-dependent actin nucleation by activating the N-WASP-WIP complex. *Cell.* 118:203–216.

Kaverina, I., T.E. Stradal, and M. Gimona. 2003. Podosome formation in cultured A7r5 vascular smooth muscle cells requires Arp2/3-dependent de-novo actin polymerization at discrete microdomains. *J. Cell Sci.* 116: 4915–4924.

Kinley, A.W., S.A. Weed, A.M. Weaver, A.V. Karginov, E. Bissonette, J.A. Cooper, and J.T. Parsons. 2003. Cortactin interacts with WIP in regulating Arp2/3 activation and membrane protrusion. *Curr. Biol.* 13:384–393.

Linder, S., and M. Aepfelbacher. 2003. Podosomes: adhesion hot-spots of invasive cells. *Trends Cell Biol.* 13:376–385.

Linder, S., D. Nelson, M. Weiss, and M. Aepfelbacher. 1999. Wiskott-Aldrich syndrome protein regulates podosomes in primary human macrophages. *Proc. Natl. Acad. Sci. USA.* 96:9648–9653.

Loisel, T.P., R. Boujemaa, D. Pantaloni, and M.F. Carlier. 1999. Reconstitution of actin-based motility of *Listeria* and *Shigella* using pure proteins. *Nature.* 401:613–616.

Lorenz, M., V. DesMarais, F. Macaluso, R.H. Singer, and J. Condeelis. 2004a. Measurement of barbed ends, actin polymerization, and motility in live carcinoma cells after growth factor stimulation. *Cell Motil. Cytoskeleton.* 57:207–217.

Lorenz, M., H. Yamaguchi, Y. Wang, R.H. Singer, and J. Condeelis. 2004b. Imaging sites of N-WASP activity in lamellipodia and invadopodia of carcinoma cells. *Curr. Biol*. 14:697–703.

McNiven, M.A., M. Baldassarre, and R. Buccione. 2004. The role of dynamin in the assembly and function of podosomes and invadopodia. *Front. Biosci.* 9:1944–1953.

Miki, H., and T. Takenawa. 2003. Regulation of actin dynamics by WASP family proteins. *J. Biochem. (Tokyo).* 134:309–313.

Miki, H., K. Miura, and T. Takenawa. 1996. N-WASP, a novel actin-depolymerizing protein, regulates the cortical cytoskeletal rearrangement in a PIP2-dependent manner downstream of tyrosine kinases. *EMBO J.* 15: 5326–5335.

Miki, H., S. Suetsugu, and T. Takenawa. 1998. WAVE, a novel WASP-family protein involved in actin reorganization induced by Rac. *EMBO J.* 17: 6932–6941.

Millard, T.H., S.J. Sharp, and L.M. Machesky. 2004. Signalling to actin assembly via the WASP (Wiskott-Aldrich syndrome protein)-family proteins and the Arp2/3 complex. *Biochem. J.* 380:1–17.

Mizutani, K., H. Miki, H. He, H. Maruta, and T. Takenawa. 2002. Essential role of neural Wiskott-Aldrich syndrome protein in podosome formation and degradation of extracellular matrix in src-transformed fibroblasts. *Cancer Res.* 62:669–674.

Moreau, V., F. Frischknecht, I. Reckmann, R. Vincentelli, G. Rabut, D. Stewart, and M. Way. 2000. A complex of N-WASP and WIP integrates signalling cascades that lead to actin polymerization. *Nat. Cell Biol.* 2:441–448.

Moreau, V., F. Tatin, C. Varon, and E. Genot. 2003. Actin can reorganize into podosomes in aortic endothelial cells, a process controlled by Cdc42 and RhoA. *Mol. Cell. Biol.* 23:6809–6822.

Mouneimne, G., L. Soon, V. DesMarais, M. Sidani, X. Song, S.C. Yip, M. Ghosh, R. Eddy, J.M. Backer, and J. Condeelis. 2004. Phospholipase C and cofilin are required for carcinoma cell directionality in response to EGF stimulation. *J. Cell Biol.* 166:697–708.

Nakahara, H., T. Otani, T. Sasaki, Y. Miura, Y. Takai, and M. Kogo. 2003. Involvement of Cdc42 and Rac small G proteins in invadopodia formation of RPMI7951 cells. *Genes Cells.* 8:1019–1027.

Neri, A., D. Welch, T. Kawaguchi, and G.L. Nicolson. 1982. Development and biologic properties of malignant cell sublines and clones of a spontaneously metastasizing rat mammary adenocarcinoma. *J. Natl. Cancer Inst.* 68:507–517.

Nicholson, R.I., J.M. Gee, and M.E. Harper. 2001. EGFR and cancer prognosis. *Eur. J. Cancer.* 37(Suppl 4):S9–S15.

Ochoa, G.C., V.I. Slepnev, L. Neff, N. Ringstad, K. Takei, L. Daniell, W. Kim, H. Cao, M. McNiven, R. Baron, and P. De Camilli. 2000. A functional link between dynamin and the actin cytoskeleton at podosomes. *J. Cell Biol.* 150:377–389.

Pollard, T.D., and G.G. Borisy. 2003. Cellular motility driven by assembly and disassembly of actin filaments. *Cell.* 112:453–465.

Rohatgi, R., P. Nollau, H.Y. Ho, M.W. Kirschner, and B.J. Mayer. 2001. Nck and phosphatidylinositol 4,5-bisphosphate synergistically activate actin polymerization through the N-WASP-Arp2/3 pathway. *J. Biol. Chem.* 276:26448–26452.

Segall, J.E., S. Tyerech, L. Boselli, S. Masseling, J. Helft, A. Chan, J. Jones, and J. Condeelis. 1996. EGF stimulates lamellipod extension in metastatic mammary adenocarcinoma cells by an actin-dependent mechanism. *Clin. Exp. Metastasis.* 14:61–72.

Snapper, S.B., F. Takeshima, I. Anton, C.H. Liu, S.M. Thomas, D. Nguyen, D. Dudley, H. Fraser, D. Purich, M. Lopez-Ilasaca, et al. 2001. N-WASP deficiency reveals distinct pathways for cell surface projections and microbial actin-based motility. *Nat. Cell Biol.* 3:897–904.

Stradal, T.E., K. Rottner, A. Disanza, S. Confalonieri, M. Innocenti, and G. Scita. 2004. Regulation of actin dynamics by WASP and WAVE family proteins. *Trends Cell Biol.* 14:303–311.

Suetsugu, S., D. Yamazaki, S. Kurisu, and T. Takenawa. 2003. Differential roles of WAVE1 and WAVE2 in dorsal and peripheral ruffle formation for fibroblast cell migration. *Dev. Cell.* 5:595–609.

Wang, W., S. Goswami, K. Lapidus, A.L. Wells, J.B. Wyckoff, E. Sahai, R.H. Singer, J.E. Segall, and J.S. Condeelis. 2004. Identification and testing of a gene expression signature of invasive carcinoma cells within primary mammary tumors. *Cancer Res.* 64:8585–8594.

Wyckoff, J., W. Wang, E.Y. Lin, Y. Wang, F. Pixley, E.R. Stanley, T. Graf, J.W. Pollard, J. Segall, and J. Condeelis. 2004. A paracrine loop between tumor cells and macrophages is required for tumor cell migration in mammary tumors. *Cancer Res.* 64:7022–7029.

Wyckoff, J.B., J.G. Jones, J.S. Condeelis, and J.E. Segall. 2000a. A critical step in metastasis: in vivo analysis of intravasation at the primary tumor. *Cancer Res.* 60:2504–2511.

Wyckoff, J.B., J.E. Segall, and J.S. Condeelis. 2000b. The collection of the motile population of cells from a living tumor. *Cancer Res.* 60:5401–5404.

Yamazaki, D., S. Suetsugu, H. Miki, Y. Kataoka, S. Nishikawa, T. Fujiwara, N. Yoshida, and T. Takenawa. 2003. WAVE2 is required for directed cell migration and cardiovascular development. *Nature.* 424:452–456.

Yanagawa, R., Y. Furukawa, T. Tsunoda, O. Kitahara, M. Kameyama, K. Murata, O. Ishikawa, and Y. Nakamura. 2001. Genome-wide screening of genes showing altered expression in liver metastases of human colorectal cancers by cDNA microarray. *Neoplasia.* 3:395–401.

Yang, Z., R. Bagheri-Yarmand, R.A. Wang, L. Adam, V.V. Papadimitrakopoulou, G.L. Clayman, A. El-Naggar, R. Lotan, C.J. Barnes, W.K. Hong, and R. Kumar. 2004. The epidermal growth factor receptor tyrosine kinase inhibitor ZD1839 (Iressa) suppresses c-Src and Pak1 pathways and invasiveness of human cancer cells. *Clin. Cancer Res.* 10:658–667.